Journal of Sound and Vibration 329 (2010) 3898–3914

Contents lists available at ScienceDirect

Journal of Sound and Vibration

journal homepage: www.elsevier.com/locate/jsvi

The vibration damping effectiveness of an active seat suspension system and its robustness to varying mass loading

I. Maciejewski [a,*], L. Meyer [b], T. Krzyzynski [a]

[a] Koszalin University of Technology, Department of Mechatronics and Applied Mechanics, Raclawicka 15-17, Koszalin 75-256, Poland
[b] Isringhausen GMBH and CO. KG, Testlaboratory, Isringhausen-Ring 58, Lemgo, 32657 DE, Germany

ARTICLE INFO

Article history:
Received 2 April 2009
Received in revised form
15 March 2010
Accepted 8 April 2010
Handling Editor: J. Lam

ABSTRACT

The paper describes the simulated dynamic response of an active vibro-isolating pneumatic suspension seat. Active control of the air-spring force is used to improve its vibro-isolation properties. For the active vibration isolating system described, a triple feedback loop control system was developed and analysed. The system robustness for different load masses was investigated using the verified active seat suspension model. The Seat Effective Amplitude Transmissibility factor (SEAT) and the maximum suspension deflection were used as the seat performance indices.

1. Introduction

Modern vibro-isolating systems use the external power supply for generating active force for the suspension system. The active force is regulated by a control system reacting to plant parameters (acceleration, velocity and displacement). Many researchers have worked on active systems in order to improve the vibro-isolating properties of active suspension systems. Research by Karnopp [1], Thompson [2] and others [3–5] has shown that it is possible to apply the principles of an active suspension to road vehicles. Authors of the papers [6–9] have demonstrated that vibration control systems utilising the pneumatic actuators can operate satisfactorily for vehicle active suspension applications. The use of actively controlled pneumatic actuators in parallel with conventional passive suspensions in order to improve ride quality has been investigated and presented in these papers.

In recent years, investigations of the active suspension have continued. For example, at the Institute of Sound and Vibration Research at the University of Southampton, the methods for simulating vibro-isolating systems and their feedback control have been developed [10,11]. The researchers from the School of Mechanical and Automotive Engineering (University of Ulsan) and from the Vibration Control Laboratory (Novosibirsk State Technical University) have worked on the minimisation of stiffness of a vibro-isolating device in order to improve its quality [12]. At the Institute of Materials and Machine Mechanics at Slovak Academy of Sciences, research on active vibration system based on a hybrid combination of the feedback and feedforward control circuits has been performed [13,14]. In the Department of Mechanical and Automation Engineering at Da-Yeh University, the principles and application of active vibration control for reducing undesired small amplitude vertical vibration are under investigation [15].

The active suspension system is a more effective vibro-isolating system but rarely used because of its high costs of construction and complicated structure. In early studies [16], the advantage of an active suspension was considered by using the "sky-hook damper" control, which applies an active force to the system. This force is proportional to the isolated

* Corresponding author. Tel.: +48 943 478 395.
E-mail addresses: igor.maciejewski@tu.koszalin.pl (I. Maciejewski), lutz.meyer@isri.de (L. Meyer), tkrzyz@tu.koszalin.pl (T. Krzyzynski).

0022-460X/$ - see front matter © 2010 Elsevier Ltd. All rights reserved.
doi:10.1016/j.jsv.2010.04.009

Nomenclature

A_{as}	surface of the air-spring, m^2
A_{ef}	effective area of the air-spring, m^2
b	critical pressure ratio
C_I	critical conductance of the inflating valve, $m^3/(s\,Pa)$
C_E	critical conductance of the exhausting valve, $m^3/(s\,Pa)$
EM3	excitation signal representative of wheel loaders
EM6	excitation signal representative of crawler loaders or crawler, dozers
F_{as}	air-spring force, N
F_{bd}	bottom end stop buffers force, N
F_{bu}	top end stop buffers force, N
F_d	shock-absorber force, N
F_{ff}	friction force, N
F_g	gravity force, N
g	gravity constant, m/s^2
h_0	initial height of the air-spring, m
k_s	static gain of the control valve, $m^3/(s\,Pa\,V)$
K_1	proportional gain of the acceleration control loop, $V\,s^2/m$
K_2	proportional gain of the relative velocity control loop, $V\,s/m$
K_3	proportional gain of the relative displacement control loop, V/m
m	suspended mass, kg
$\overline{m}$	nominal value of the suspended mass, kg
m_{as0}	initial air mass inside the air-spring, kg
m_s	mass of suspension system affixed to suspended mass, kg
$\dot{m}_I$	mass flow rate for inflating of the air-spring, kg/s
$\dot{m}_E$	mass flow rate for exhausting of the air-spring, kg/s
p_{as}	air pressure inside the air-spring, Pa
p_s	air pressure of the power supply, Pa
p_0	atmospheric pressure, Pa
R	gas constant, $J/(kg\,K)$
RMS	root-mean-square value
SEAT	Seat Effective Amplitude Transmissibility factor
t_0	time constant of the control valve, s
T_s	air temperature of the power supply, K
T_{as}	air temperature inside the air-spring, K
T_{norm}	temperature of standard conditions, K
T_w	wall temperature of the air-spring, K
T_0	atmospheric air temperature, K
u	overall control voltage, V
u_I	control voltage of the inflating valve, V
u_E	control voltage of the exhausting valve, V
u_{max}	maximum value of the overall control voltage, V
u_{min}	minimum value of the overall control voltage, V
WNP	excitation signal similar to white, band limited noise
V_{as}	air-spring volume, m^3
x	displacement of the suspended mass, m
$\ddot{x}$	acceleration of the suspended mass, m
x_s	displacement of the excitation, m
$(x-x_s)_{max}$	maximum relative displacement of the suspension system (peak to peak value), m
$\ddot{x}_{set}$	setting value of the acceleration control loop, m/s^2
$(x-x_s)_{set}$	setting value of the relative displacement control loop, m
$(\dot{x}-\dot{x}_s)_{set}$	setting value of the relative velocity control loop, m/s
α_{as}	overall heat transfer coefficient of the air-spring, $W/(m^2\,K)$
Δ_m	variations of the value of suspended mass
δ_{as}	reduction ratio of the air-spring
κ	adiabatic coefficient
ρ_{norm}	density of standard conditions, kg/m^3

absolute velocity of the mass. Subsequently, the structure of active systems has been mainly based on the linear-quadratic-Gaussian control (LQG control) technique [17] for determining the optimal control to minimise a performance index. The performance index has two contributions: firstly, to bring the controlled variable to zero (minimising the error) and secondly, to keep the control input as small as possible. The LQG control can be used to obtain the global overview of all possible optimal solutions for a defined trade-off between regulation performance and the control effort. The selection of a specific solution would then be only possible with a method which could accept many additional criteria and constraints, in addition to the conventional LQG settings.

In both the "sky-hook" and LQR methods the plant was assumed to be a linear or approximately linear system. However, many suspension systems are rather complicated and their models should take into account the nonlinearity and uncertainties of the plant dynamics. Recently, various kinds of active suspension systems have been considered for such complicated systems using the nonlinear control, the adaptive control, the predictive control and the robust control, etc. The fuzzy-logic control [18,19] allows the creation of the nonlinear regulators functioning with minimal knowledge about the system dynamics. The neural network control [20,21] helps to adapt the active system behaviour to different working conditions and also to predict the excitation conditions in the future time. The H-inf control [22,23] is frequently discussed in the context of robustness and disturbance attenuation of an active suspension.

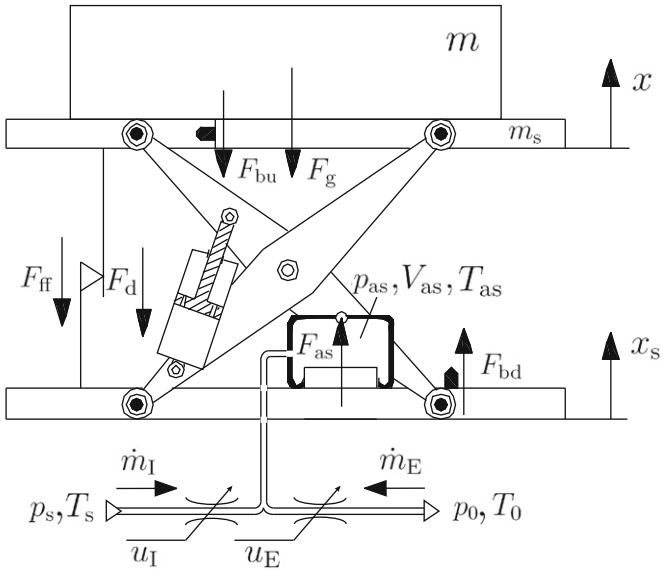

Fig. 1. Physical model of the active seat suspension.

Nonlinear active suspension systems provide more effective vibration isolation performance, but require more complicated control systems than linear active suspension systems based on "sky-hook damper" or LQG control theory. The ongoing development of control algorithms indicates that improved methods of controlling active suspension systems are an effective way to deal with the conflicting suspension system performance problem [24].

The purpose of this paper is to present an effective way of modelling and controlling the vibro-isolating properties of an active seat suspension system in response to varying load mass.

2. Modelling of the active seat suspension with an air-spring

2.1. Physical and mathematical model

In Fig. 1 a physical model of the active seat suspension system containing an air-spring and a hydraulic shock-absorber was shown. This system used the active air-flow to the air-spring (inflating and exhausting) and was regulated by the controller and proportional directional control valves. The proportional valves have an unlimited number of stable states that are proportional to the analogue input signal obtained from the controller [26]. The proportional flow control valves were used in the active seat suspension system and therefore the mass flow rates $\dot{m}_I$ and $\dot{m}_E$ were proportional to the voltage input signal u_I and u_E, respectively. Inflating the air-spring was carried out by an external air compressor and the exhaust of the air-spring was released directly to the atmosphere. The air-flow changed the air pressure inside the air-spring and the variation of pressure created an active force for the suspension system.

The equation of the motion of the active seat suspension took a similar form as in the case of the passive seat suspension model as shown in the authors' previous paper [25]:

$$(m+m_s)\ddot{x} = F_{as}+F_d+F_{ff}+F_b+F_g \tag{1}$$

where m is the suspended mass and m_s is the mass of suspension system affixed to the suspended mass. The mathematical models of the basic forces in the system, the spring force F_{as}, the damping force F_d, the forces from end-stop buffers: bottom F_{bd} and top F_{bu}, the overall friction force of suspension system F_{ff} and the gravity force of suspended mass F_g, were sufficient for modelling the forces in the passive system. However, the actual value of air pressure p_{as} in the air-spring was different from the passive seat suspension model because the air-spring was inflated and exhausted. The mass flow rates during inflating and exhausting were controlled proportionally to the electric input signals.

The differential equation for the pressure dynamics in the air-spring chamber as a function of the mass flow rates was given by [26,27]

$$\dot{p}_{as}V_{as}+\kappa p_{as}\dot{V}_{as}+(\kappa-1)A_{as}\alpha_{as}(T_{as}-T_w) = \kappa R(\dot{m}_I T_s-\dot{m}_E T_{as}) \tag{2}$$

where V_{as} is the air-spring volume, κ is the adiabatic coefficient (assumed equal to 1.4), A_{as} is the wall surface of the air-spring, α_{as} is the heat transfer coefficient across the air-spring wall calculated in reference to [27], T_w is the wall temperature estimated as equal to the ambient temperature, R is the gas constant and T_s is the temperature of inflowing air. In Eq. (2) the heat transfer through the boundaries of the pneumatic capacity was also taken into account.

The simplified model of the air-spring volume was described as the cylinder configuration:

$$V_{as} = A_{ef}\left(\frac{x-x_s}{\delta_{as}} + h_0\right) \tag{3}$$

where A_{ef} is the effective area of the air-spring, δ_{as} is the reduction ratio of the air-spring motion, h_0 is the initial height of the air-spring, respectively. The reduction ratio δ_{as} was calculated on the basis of kinematics of the shear guidance mechanism as a quotient between the suspension system motion and the air-spring motion in vertical direction.

The air temperature T_{as} in the air-spring was calculated from its actual pressure, the variable air-spring volume and the initial mass of air m_{as0}, with the assistance of ideal gas law:

$$T_{as} = \frac{p_{as}V_{as}}{m_{as0} + \int(\dot{m}_I - \dot{m}_E)\,dt} \tag{4}$$

where $\dot{m}_I - \dot{m}_E$ describes the differential mass flow rate between inflating and exhausting of the air-spring. If the net value of integral in the denominator of Eq. (4) was nonzero then the air spring inflation or deflation was obtained (except of temperature changes in the air-spring). That resulted in the possibility of the change in the suspension system static position. Therefore, the height of the active seat had to be controlled in order to keep the suspension system in static position (see Section 2.2).

A description of the mass flow rate contains the critical conductances: for inflating C_I and for exhausting C_E of the air-spring and critical pressure ratio b as its parameters [28]. The mass flow rate of inflated air into the air-spring was calculated as follows (subcritical range $p_{as}/p_s > b$):

$$\dot{m}_I = C_I p_s \rho_{norm}\sqrt{\frac{T_{norm}}{T_s}}\sqrt{1-\frac{\left(\frac{p_{as}}{p_s}-b\right)^2}{(1-b)^2}} \tag{5}$$

and in the supercritical range ($p_{as}/p_s \le b$):

$$\dot{m}_I = C_I p_s \rho_{norm}\sqrt{\frac{T_{norm}}{T_s}} \tag{6}$$

whereas the mass flow rate of exhausted air from the air-spring was calculated as follows (subcritical range $p_0/p_{as} > b$):

$$\dot{m}_E = C_E p_{as} \rho_{norm}\sqrt{\frac{T_{norm}}{T_{as}}}\sqrt{1-\frac{\left(\frac{p_0}{p_{as}}-b\right)^2}{(1-b)^2}} \tag{7}$$

and in the supercritical range ($p_0/p_{as} \le b$):

$$\dot{m}_E = C_E p_{as} \rho_{norm}\sqrt{\frac{T_{norm}}{T_{as}}} \tag{8}$$

where ρ_{norm} and T_{norm} are the ISO standard values [28].

The first-order differential equations were used to describe the conductances C_I and C_E of the proportional directional control valves as a function of the control signals: for inflating u_I and for exhausting u_E of the air-spring. The proportional directional control valves were described simply as the first inertial elements in order to model their actuating time only (typically 5 ms). Hysteresis effects of the control valves were not taken into account. The high performance pneumatic valve used was very precise that has been reflected in a low hysteresis (below 0.4 percent). Using these assumptions the equations were given by [26]

$$t_0\dot{C}_I + C_I = k_s u_I, \quad t_0\dot{C}_E + C_E = k_s u_E \tag{9}$$

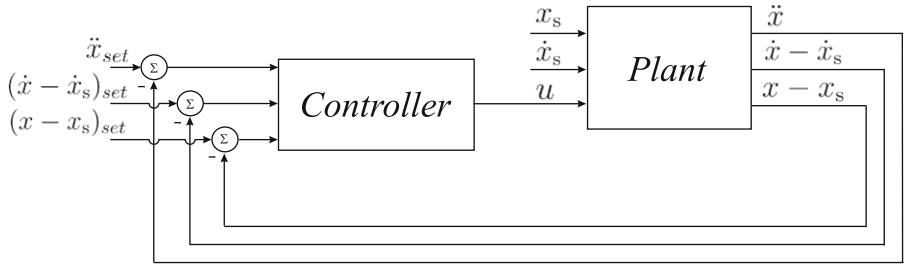

Fig. 2. Control system of the active seat suspension.

where t_0 is the time constant of control valve and k_s is the static gain of control valve, respectively. In this paper the air-spring inflation and deflation was achieved by using proportional flow control valves of the same dynamic properties.

2.2. Control principle of the active seat suspension

The control system of the active seat suspension used a triple feedback loop: the acceleration of vibro-isolated mass $\ddot{x}$, the relative velocity of suspension system $\dot{x}-\dot{x}_s$ and the relative displacement of suspension system $x-x_s$ (Fig. 2). The control policy was formulated as

$$u = K_1(\ddot{x}_{set}-\ddot{x})+K_2((\dot{x}-\dot{x}_s)_{set}-(\dot{x}-\dot{x}_s))+K_3((x-x_s)_{set}-(x-x_s)) \quad (10)$$

where K_1 is the proportional gain of acceleration loop, K_2 is the proportional gain of relative velocity loop and K_3 is the proportional gain of relative displacement loop, respectively.

Subsequently, the continuous control signal u was divided into two signals. The positive part of signal u_I controlled the inflow to the air-spring and the negative part of signal u_E controlled the outflow from the air-spring. Additionally, the

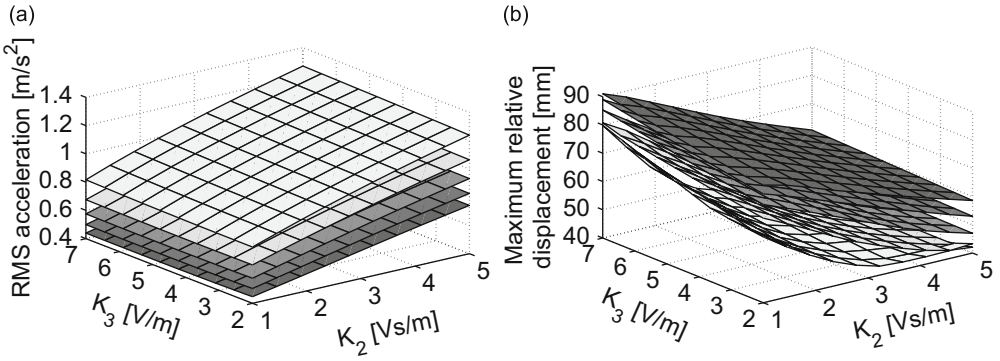

Fig. 3. Effective value of the suspended mass acceleration (a) and maximum relative displacement of the suspension system (b) for different gain of a triple feedback loop control system: $K_1 = 0.2\,\mathrm{V\,s^2/m}$ ( ), $K_1 = 0.3\,\mathrm{V\,s^2/m}$ ( ), $K_1 = 0.4\,\mathrm{V\,s^2/m}$ ( ), $K_1 = 0.5\,\mathrm{V\,s^2/m}$ ( ), $K_1 = 0.6\,\mathrm{V\,s^2/m}$ ( ).

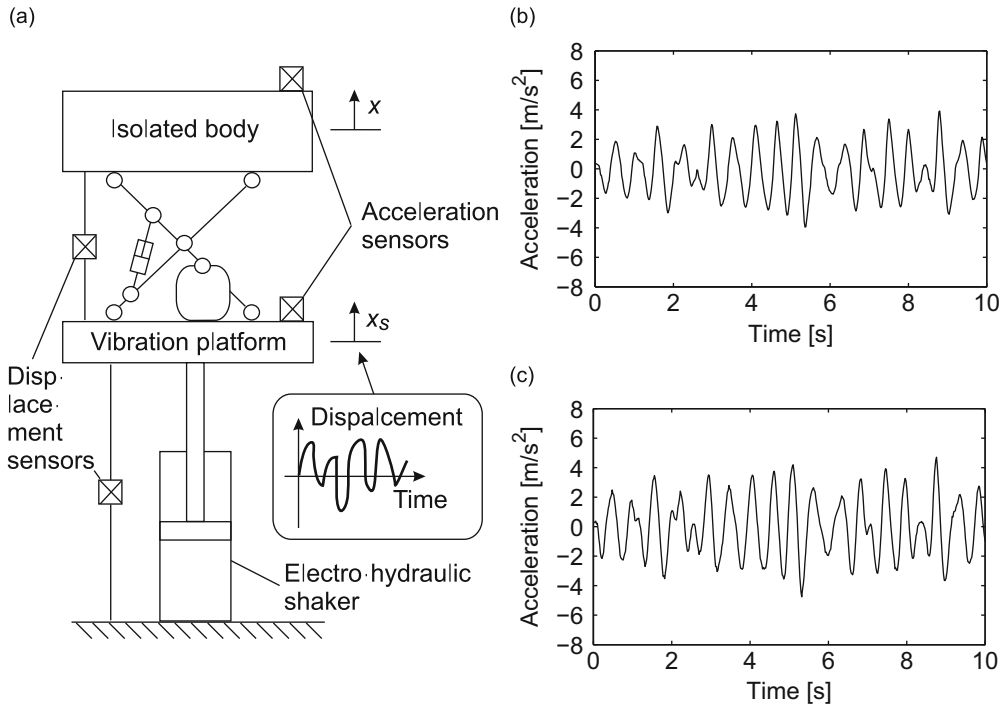

Fig. 4. Experimental set-up for the evaluation of the suspension dynamical behaviour (a), measured acceleration of the isolated body (b), measured acceleration of the vibration platform (c).

Table 1
Numerical values of the cut-off frequencies, filter orders and maximum magnitudes for the excitation signals WNP, EM3 and EM6.

Excitation signal	High-pass filter		Low-pass filter		Maximum magnitude (m^2/s^3)
	Cut-off frequency (Hz)	Filter order	Cut-off frequency (Hz)	Filter order	
WNP	0.7	4	8	2	0.4
EM3	1.5	4	3	4	1.75
EM6	6.5	2	9	2	0.35

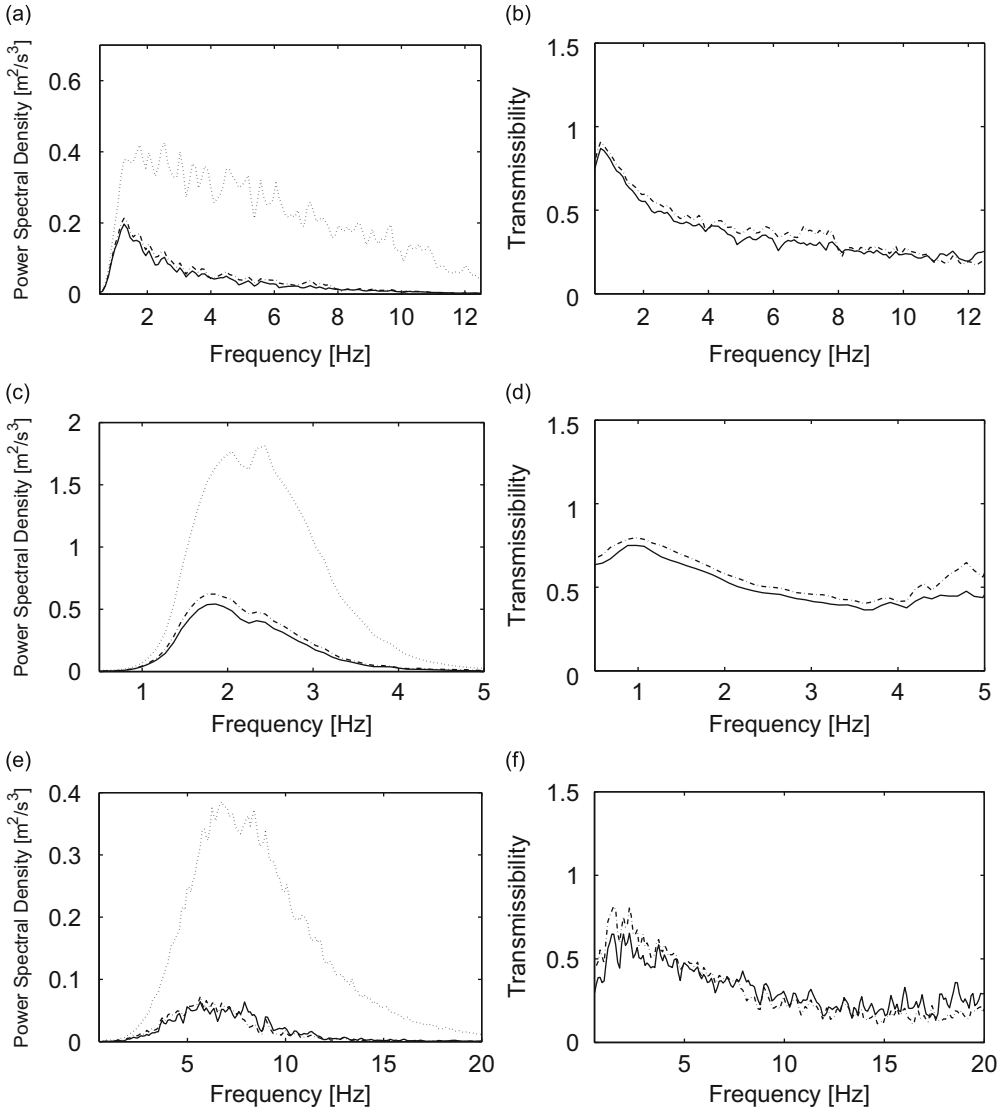

Fig. 5. Measured (-·-·-) and simulated (—) power spectral densities for the excitation signals (·····): (a) WNP, (c) EM3, (e) EM6 and transmissibility curves of the active seat suspension for the excitation signals: (b) WNP, (d) EM3, (f) EM6.

deadbands in the signal flow were modelled. If the defined control range $\langle u_{\min}; u_{\max} \rangle$ was exceeded, then the control signal was saturated:

$$u_I = \begin{cases} 0 & \text{for } u \le 0, \\ u & \text{for } 0 < u < u_{\max}, \\ u_{\max} & \text{for } u \ge u_{\max}, \end{cases} \quad u_E = \begin{cases} 0 & \text{for } u \ge 0 \\ -u & \text{for } u_{\min} < u < 0 \\ -u_{\min} & \text{for } u \le u_{\min} \end{cases} \tag{11}$$

With such kind of the control system it was possible to minimise both of vibro-isolation criteria, which have been opposite to each other [29]: the acceleration acting on an operator $\ddot{x}$ and the maximum relative displacement of suspension system $(x-x_s)_{max}$, simultaneously. Each parameter value used by the seat suspension model was shown in Appendix A.

2.3. Controller settings variation

The influence of controller settings on the dynamic behaviour of the active seat suspension was performed with the assistance of numerical simulation. The seat suspension model was excited by a white noise signal and the variations of controller settings were taken into account over the following ranges:

- the proportional gain of the acceleration loop K_1 = 0.2–0.6 V s^2/m,
- the proportional gain of the relative velocity loop K_2 = 1–5 V s/m,
- the proportional gain of the relative displacement loop K_3 = 1–7 V/m.

In Fig. 3 the effective acceleration (RMS) of the isolated mass and the maximum relative displacement of the suspension system for different gains of the triple feedback loop control system were shown.

The obtained results (Fig. 3) confirmed that the decrease of acceleration $\ddot{x}$ acting on the suspended mass has the effect of increasing the maximum relative displacement $(x-x_s)_{max}$ of the suspension system and vice versa. The first estimation of controller settings: $K_1 = 0.4\,\mathrm{V\,s^2/m}$, $K_2 = 2.22\,\mathrm{V\,s/m}$, $K_3 = 4.44\,\mathrm{V/m}$ effectively dealt with the conflicting suspension system performance problem [29]. Moreover, the proposed control system, with correctly selected controller settings, made the dynamic behaviour of the active seat highly insensitive for the different load masses.

2.4. Model verification

For the purpose of this paper, the dynamic behaviour of the suspension system was modelled in the MATLAB – Simulink® software package. The equations (Eqs. (1)–(11)) were programmed using the interactive graphical environment, which allowed to simulate and test a variety of the time-varying system. The nonlinear ordinary differential equations (ODE) in the model were solved numerically using the fixed-step (step time of 1 ms) Bogacki–Shampine solver [30].

The experimental investigations were performed using the test set-up shown in Fig. 4. The suspension system was mounted on the vibration platform, initially loaded and excited by the electro-hydraulic shaker. The dynamic behaviour of the active seat suspension system was verified for the excitation signals: WNP—a signal similar to the white noise, band limited noise in the range of frequency 1–12.5 Hz, EM3—a signal with relatively low frequencies and high amplitudes of vibration (representative of wheel loaders [31]), EM6—a signal with higher frequencies and lower amplitudes of vibration (representative of caterpillar machines [31]).

The excitation signals in time domain were obtained using a signal generator with the random wave form. Spectral properties of the generated signals were close to the white noise signal (magnitude of the power spectral density function was constant). Subsequently, their spectral characteristics were formed by the Butterworth filters: high-pass and low-pass. The cut-off frequencies, filter orders and maximum magnitudes of the power spectral density functions were shown in Table 1. The frequency characteristics of the excitation signals were demonstrated in Fig. 5a, c, e.

The measured and simulated signals were the acceleration of the vibration platform, the acceleration of the isolated body, the relative displacement of the suspension system and the absolute displacement of the vibration platform. Based on the acceleration signals coming from the vibration platform and suspended mass, the power spectral densities and transmissibility functions were evaluated. The simulation and experimental results for selected excitation signal were shown in Fig. 5.

The simulation results of the active seat suspension system satisfactorily corresponded to the results measured experimentally. The best agreement of the seat effective amplitude transmissibility factor and the maximum relative displacement of suspension system was observed at the excitation signal called WNP and EM6. A lower agreement was

Table 2
Simulated and measured SEAT factors, maximum relative displacements and relative errors of the active seat suspension for the excitation signals: WNP, EM3, EM6.

	Simulation		Measurement		Relative error	
	SEAT factor	Maximum relative displacement (mm)	SEAT factor	Maximum relative displacement (mm)	SEAT factor (%)	Maximum relative displacement (%)
WNP	0.356	69	0.392	69	9	0
EM3	0.491	74	0.532	76	8	3
EM6	0.349	13	0.347	12	1	8

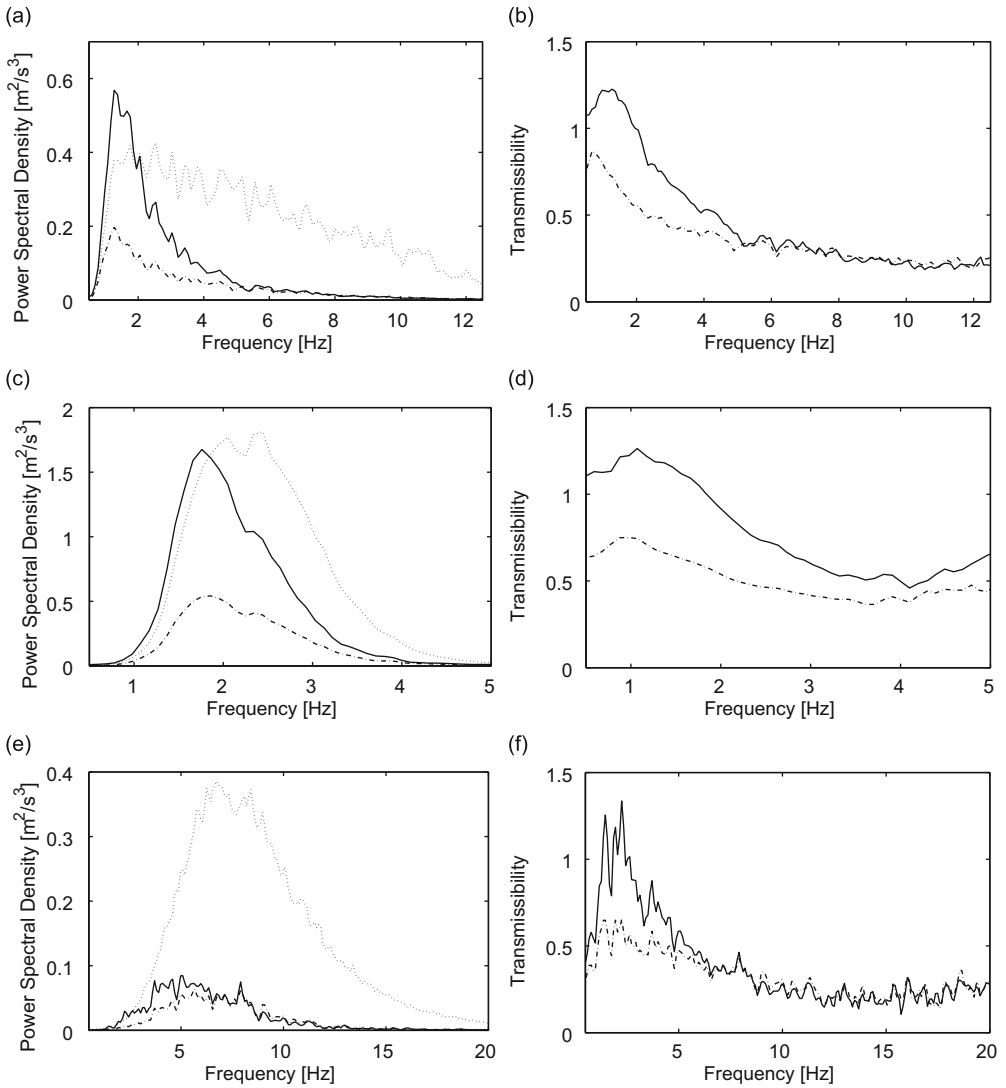

Fig. 6. Simulated power spectral densities for the excitation signals (·····): (a) WNP, (c) EM3, (e) EM6 and transmissibility curves of the passive (—) and active (-·-·-) seat suspensions for the excitation signals: (b) WNP, (d) EM3, (f) EM6.

Table 3
Simulated SEAT factors, maximum relative displacements and improvements of the active seat suspension in comparison with the passive suspension for the excitation signals: WNP, EM3, EM6.

	Passive		Active		Improvement	
	SEAT factor	Maximum relative displacement (mm)	SEAT factor	Maximum relative displacement (mm)	SEAT factor (%)	Maximum relative displacement (%)
WNP	0.484	71	0.356	69	26	3
EM3	0.766	84	0.491	74	36	12
EM6	0.389	10	0.349	13	10	−30

shown for EM3 excitation signal. The particular Seat Effective Amplitude Transmissibility factors (SEAT) [31,32] maximum relative displacements and relative errors were presented in Table 2.

The Seat Effective Amplitude Transmissibility factor (SEAT) provides a simple numerical assessment of the seat isolation efficiency. The SEAT factor was defined as the quotient of frequency weighted root mean square value of the seat and input accelerations [31]. The frequency weighting of acceleration signal should be performed in accordance with the procedure presented in [32]. The SEAT factor value of 1 means that seating on the working machine cabin floor would produce the

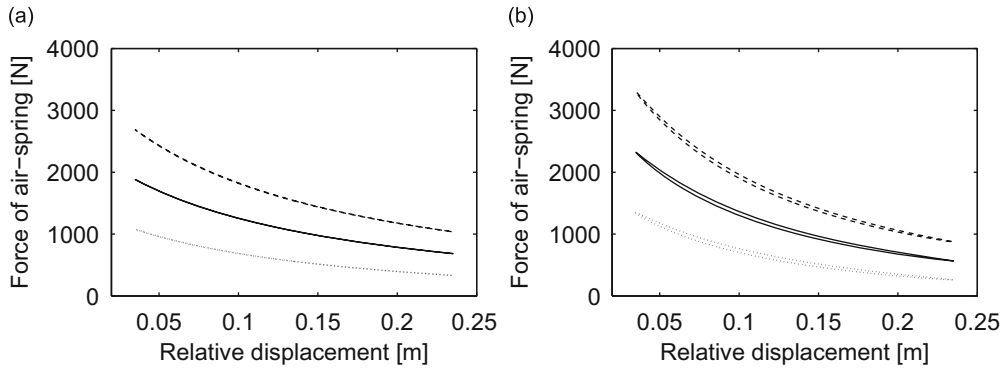

Fig. 7. Force of the air-spring for different masses loading the suspension system: $m=50$ kg (-·-·-), $m=100$ kg (—), $m=150$ kg (·····) at the frequencies of sinusoidal excitation signal: (a) 0.001 Hz, (b) 1 Hz.

same vibration discomfort. If the SEAT factor value is grater than 1, the vibration discomfort is increased by the seat. If the SEAT factor value is less than 1, the useful vibro-isolation is provided by the seat [33].

3. Improvement in suspension vibration damping effectiveness by active control

The active seat suspension system decreased the maximum vibration amplitudes at the resonance frequency of a corresponding passive suspension by about 50 percent. The active seat reduced the vibration transmission over the whole frequency range investigated. The power spectral density curves of the active suspension system were lower than the power spectral density of excitation signal over the full frequency range, so the transmissibility curve was also lower than 1 over the full range (Fig. 6).

The Seat Effective Amplitude Transmissibility factors (SEAT) [31,32] for the active suspension system were lower than SEAT factors for the passive system. Therefore, the vibrations transmitted to the isolated mass were reduced for all excitation signals. The active system was more efficient in reducing the isolated body acceleration for the challenging EM3 excitation signal which had relatively low frequencies and high amplitudes of vibration. Moreover, the maximum deflection of the suspension system was decreased for this kind of input signal at the low air-power supply requirement (the compressed air consumption of about 50 Nl/min (normal liters per minute)). The active system was too slow for the higher frequency vibration energy content of the EM6 excitation, therefore its efficiency was lower. The SEAT factors, maximum relative displacements and relative errors were presented in Table 3.

The increase of the suspension damping effectiveness was achieved by inflating/exhausting of the pneumatic spring. In such solution, pressure in the pneumatic spring was changing, so the active force in the suspension system was provided. The triple feedback loop control system significantly influenced vibration control in the frequency bandwidth 0.5–4 Hz. The effects of the absolute acceleration feedback loop were evidently shown in Fig. 6. The relative velocity feedback loop mainly reduced the suspension deflection (Table 3) and the relative displacement feedback loop contributed to keeping the static position of the suspension system. The advantage of such control is the attenuation of resonant frequency vibration without the amplification of high frequency vibration.

4. Robustness of the passive and active suspension systems

Robustness in control system design was required because of the sensitivity of the real engineering systems to external disturbance. There are always differences between mathematical models used for design and the real system. Most often the uncertainties of a controlled system come from disturbance signals, unmodelled plant dynamics, neglected nonlinearities in the modelling and plant parameter variations. A successfully designed control system should always be able to work smoothly in spite of the uncertainties of system dynamics as well as any unforeseeable exceptional situations in working conditions.

4.1. Source of the seat suspension system uncertainty

The passive seat suspension is sensitive to changes in its working conditions. The static and dynamic behaviour of the system depended on the mass m loading the suspension, because the suspension system spring force F_{as} was a function of the pressure inside the air-spring [26]:

$$F_{as}=\frac{\kappa A_{ef}}{\delta_{as}V_{as}}\int\left(-p_{as}\dot{V}_{as}-\frac{\kappa-1}{\kappa}A_{as}\alpha_{as}(T_{as}-T_w)\right)\mathrm{d}t+(m+m_s)g \tag{12}$$

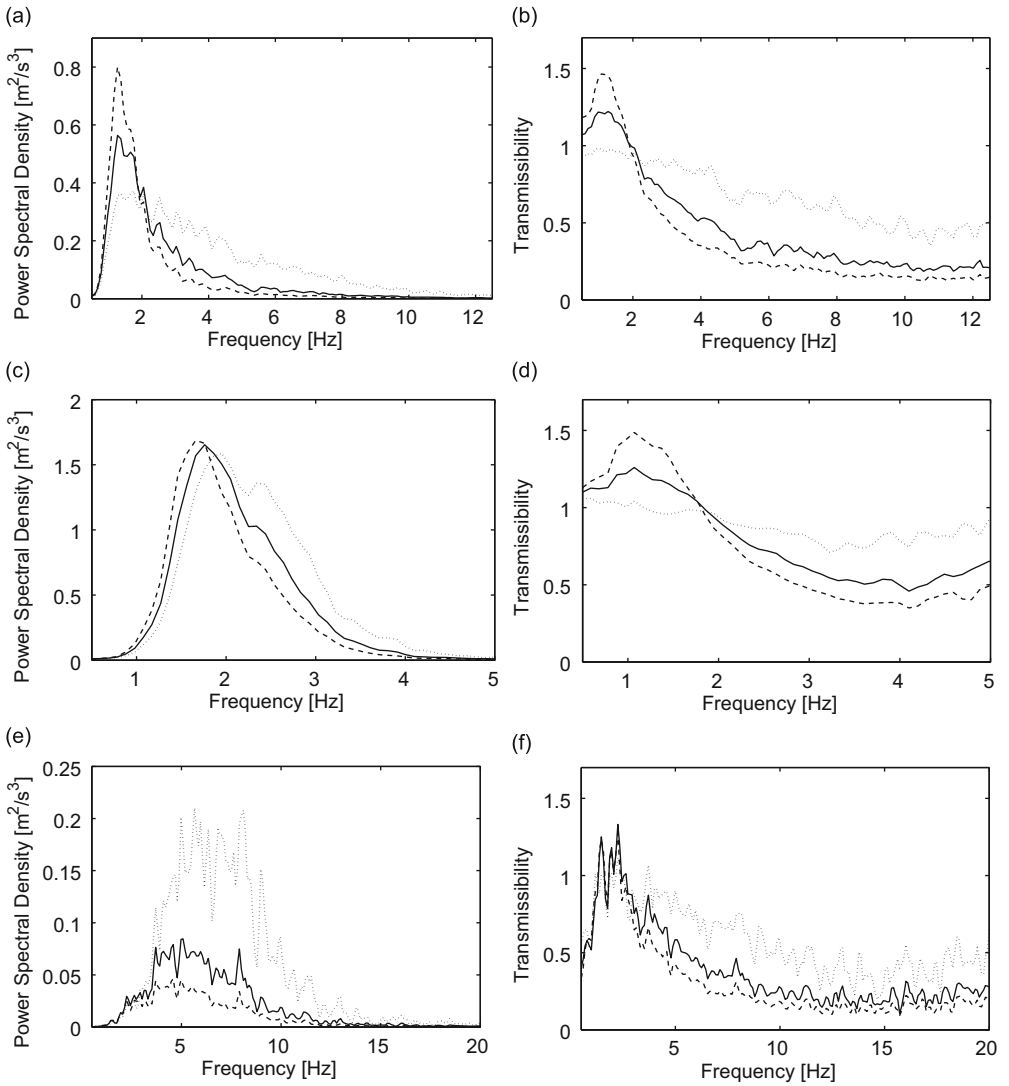

Fig. 8. Simulated power spectral densities for excitation signals: (a) WNP, (c) EM3, (e) EM6 and transmissibility curves of passive seat suspension for excitation signals: (b) WNP, (d) EM3, (f) EM6 at different variations of the value of mass: $\Delta_m = -0.5$ (·····), $\Delta_m = 0$ (—), $\Delta_m = 0.5$ (·····).

The forces of the air-spring at the different loads of suspension system were shown in Fig. 7. Such simulation results were obtained for sinusoidal motion of suspension system at the same displacement amplitude of excitation signal (0.1 m) and two frequencies: 0.001 Hz (Fig. 7a) and 1 Hz (Fig. 7b).

The stiffness of the suspension system was nonlinear in the relative displacement domain and its characteristic had a dissimilar shape in the case of different loading masses. The variable stiffness caused the nonconstant eigenfrequency of vibration isolating system. That resulted in differing vibro-isolating properties of the passive seat suspension system for different weights of machine operator. The active seat should ensure the same vibration isolating properties of the suspension system for each operator.

4.2. Parametric uncertainty of the seat suspension model

The parametric uncertainties are very often used for modelling the system dynamic perturbations, such as the inaccurate description of component characteristics, the shifting of operating points, etc. This kind of uncertainty may be modelled by varying the nominal system parameter values over some practically achievable ranges. In the present study, the parametric uncertainty of the passive and active seat suspension models is described as follows [34]:

$$m = \overline{m}(1+\Delta_m) \quad \text{for } -0.5 \le \Delta_m \le 0.5 \tag{13}$$

where $\overline{m}$ is the nominal value of mass loaded the suspension system and Δ_m represent the possible variations of the value of mass.

4.3. System robustness of the passive seat suspension

The power spectral densities of the acceleration and transmissibility curves of the simulated passive suspension system for variations of the value of mass $-0.5 \le \Delta_m \le 0.5$ were shown in Fig. 8. The change of model parameter m influences the dynamic behaviour of passive seat suspension. The suspension system loaded with a high mass ($\Delta_m = 0.5$) caused amplification of vibration at the resonance frequency, but for higher frequencies, where the suspension was isolating, that system had the best vibro-isolating properties of all the cases considered. The system loaded with a low mass ($\Delta_m = -0.5$) had much lower amplification of vibration at resonance, but its vibration isolating properties at higher frequency range were poor. In summary, the system robustness of the passive seat suspension for changeable machine operator weight was unsatisfactory.

4.4. System robustness of the active seat suspension

The power spectral densities of acceleration and transmissibility curves of the simulated active suspension system for variations of the value of the mass $-0.5 \le \Delta_m \le 0.5$ were shown in Fig. 9. The dynamic behaviour of the active seat

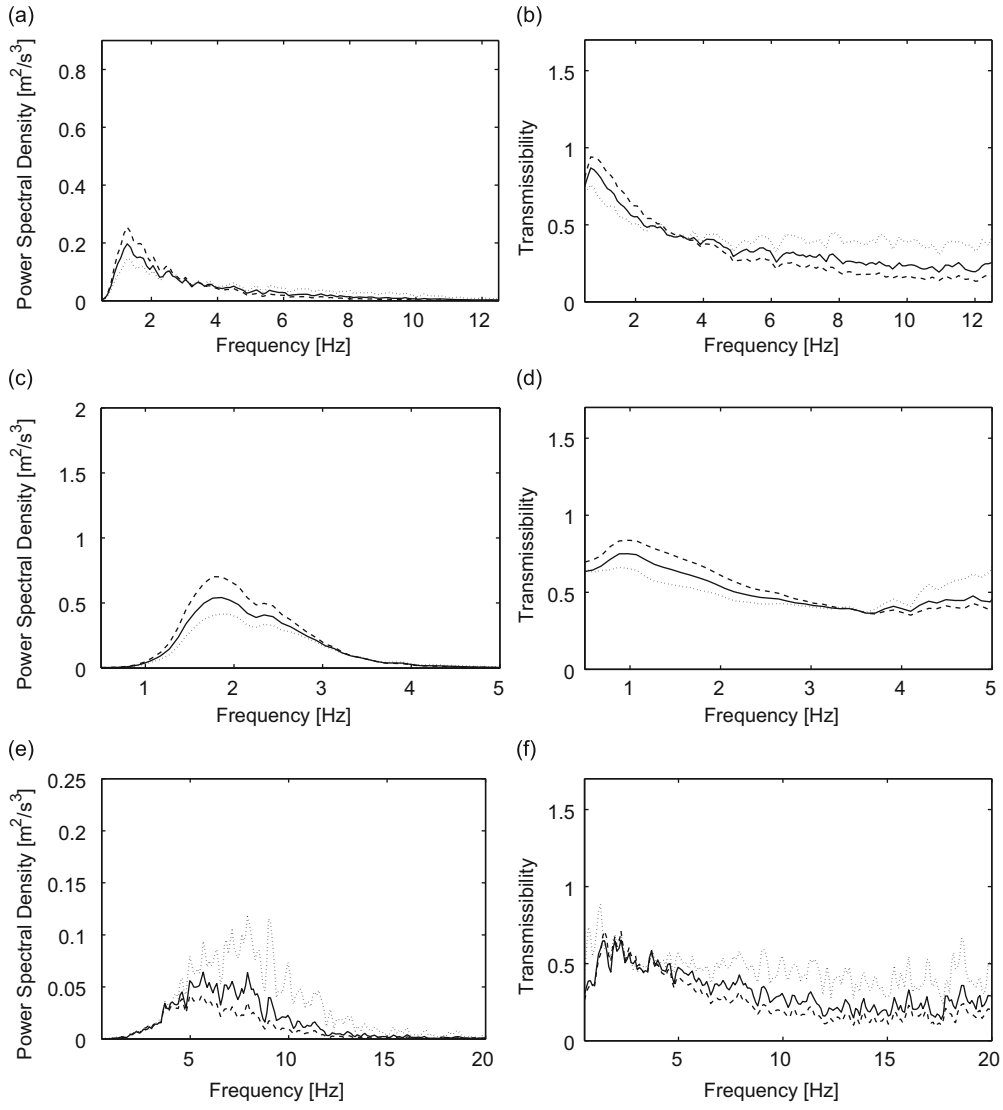

Fig. 9. Simulated power spectral densities for excitation signals: (a) WNP, (c) EM3, (e) EM6 and transmissibility curves of active seat suspension for excitation signals: (b) WNP, (d) EM3, (f) EM6 at different variations of the value of mass: $\Delta_m = -0.5$ (·····), $\Delta_m = 0$ (—), $\Delta_m = 0.5$ (·····).

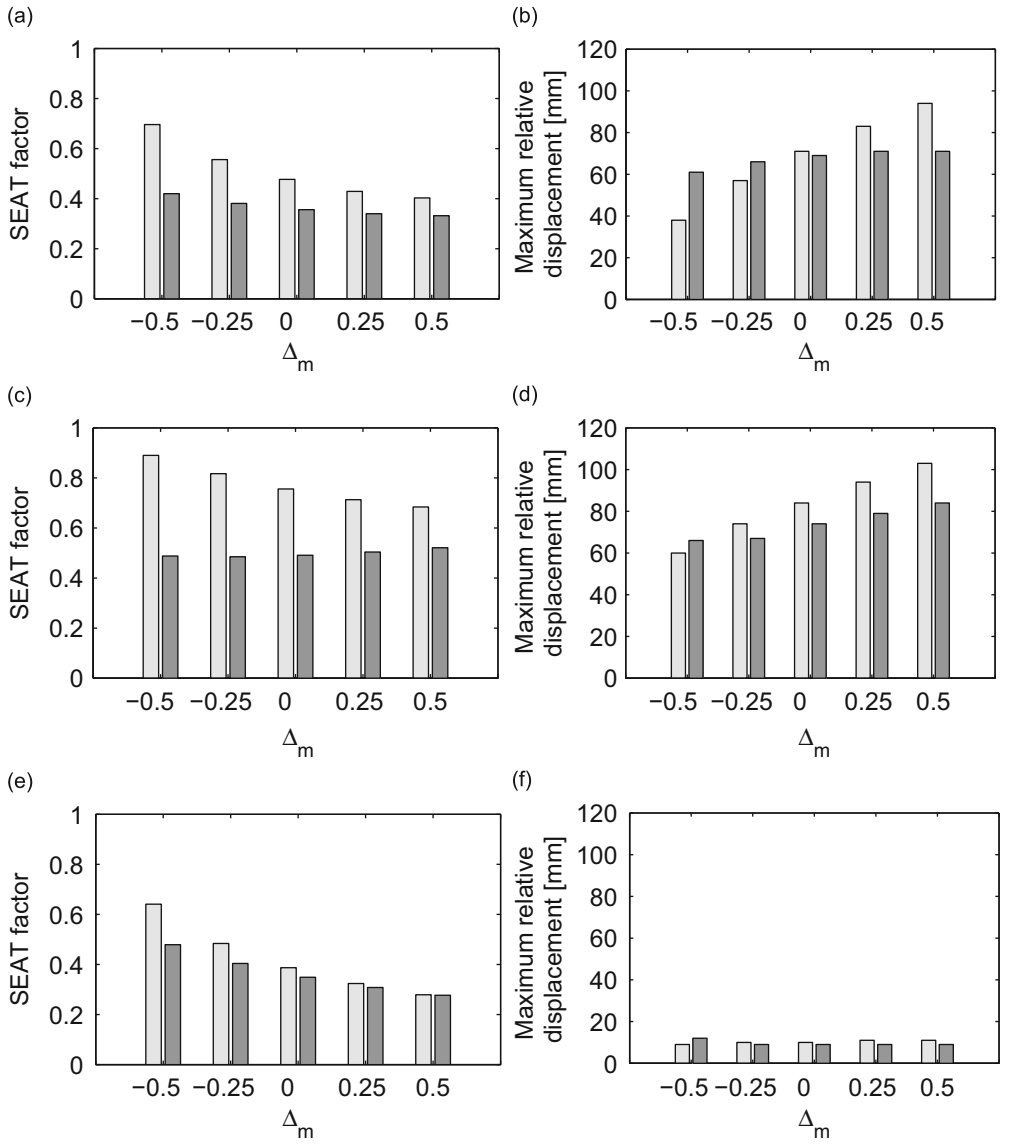

Fig. 10. Simulated SEAT factors for the excitation signals: (a) WNP, (c) EM3, (e) EM6 and maximum relative displacements of the passive ( ) and active ( ) seat suspensions for the excitation signals: (b) WNP, (d) EM3, (f) EM6 at different variations of the value of mass.

Table 4
Percent variation of the SEAT factor and of the maximum relative displacement in respect to $\pm 50\%$ variation of the nominal value of the suspended mass for excitation signals: WNP, EM3, EM6.

	Passive		Active	
	ΔSEAT (%)	$\Delta(x-x_s)_{max}$ (%)	ΔSEAT (%)	$\Delta(x-x_s)_{max}$ (%)
WNP	61	78	25	16
EM3	27	51	7	24
EM6	94	20	57	33

suspension loaded by a high mass ($\Delta_m = 0.5$) and low mass ($\Delta_m = -0.5$) were much closer to each other than the corresponding behaviour of the passive seat suspension (Fig. 9). The main improvement of the system robustness was observed in the frequency range 0.5–4 Hz. In that frequency range the air-flow effectively controlled the air-spring force. At higher frequencies (more than 4 Hz) the shock-absorber force and the friction force were dominant. In that frequency range both systems, the passive suspension and the active suspension, gave almost the same response.

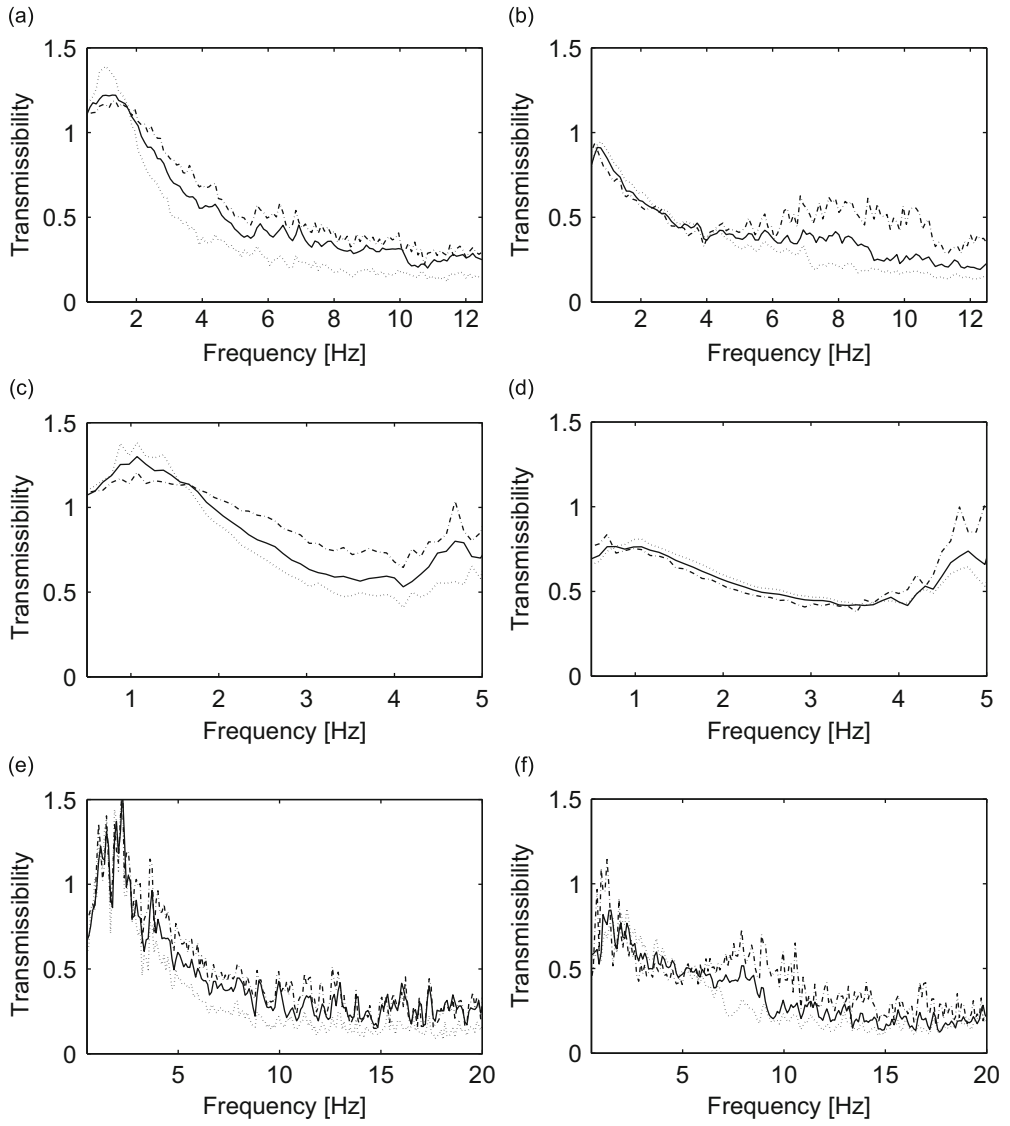

Fig. 11. Measured transmissibility curves of passive seat suspension loaded by mass 50 kg (-·-·-), 80 kg (—) and 120 kg (·····) for excitation signals: (a) WNP, (c) EM3, (e) EM6 and active seat suspension loaded by mass 50 kg (-·-·-), 80 kg (—) and 120 kg (·····) for excitation signals: (b) WNP, (d) EM3, (f) EM6.

4.5. Comparison of both systems vibration damping performance

The simulated SEAT factors and maximum relative displacements of the passive and active seat suspensions with different variations of the value of mass Δ_m were shown in Fig. 10. The results show that the system robustness in response to a load mass change was higher in the case of the active seat than when it comes to the passive seat. Moreover, in the case of the active seat the SEAT factor and the maximum relative displacement for excitation signals WNP and EM3 were nearly independent of mass loading, whereas in the case of the passive seat the dynamic behaviour of the seat strongly depended on its mass load. Regarding the passive system, the increase of load mass resulted in decreasing the SEAT factor but also in increasing the maximum relative displacement of the seat suspension. For the excitation signal EM6, the vibro-isolation effectiveness of the active seat suspension was only insignificantly higher than of the passive seat.

The performance robustness of the active system was also expressed in a numerical form, i.e. the percentage variation of the SEAT factor and of the maximum relative displacement in respect of ± 50 percent variation of the nominal value of the suspended mass. Their percentage values provided a simple numerical assessment of the suspension system performance robustness for different load masses. The ΔSEAT and $\Delta(x{-}x_s)_{\max}$ values of 0 percent mean that the active seat suspension dynamic behaviour was totaly unsensitive for different load masses. If the values ΔSEAT and $\Delta(x{-}x_s)_{\max}$ increased then the seat suspension was more sensitive to different load masses. The numerical values of ΔSEAT and $\Delta(x{-}x_s)_{\max}$ for the WNP, EM3 and EM6 excitation signals were presented in Table 4.

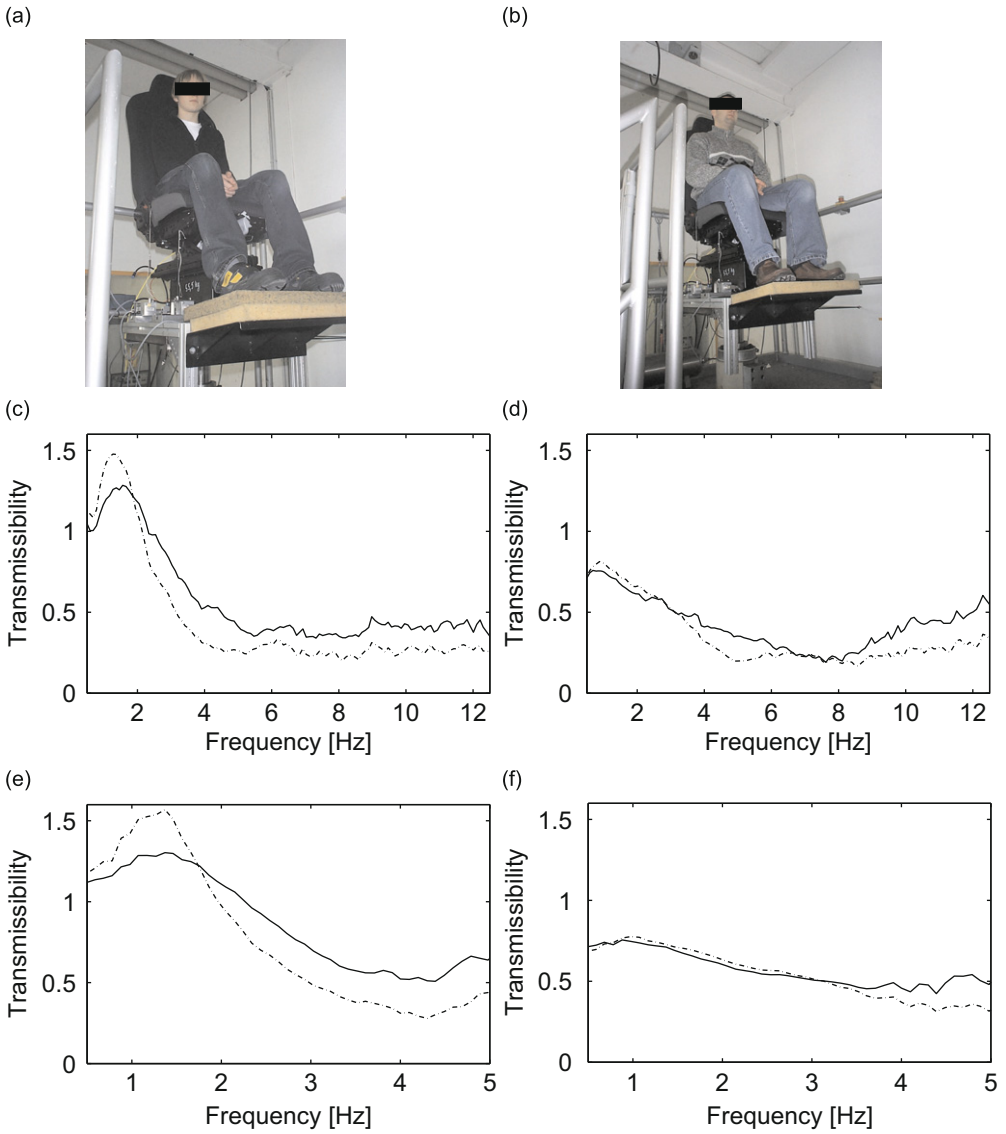

Fig. 12. Test person: (a) body mass 55 kg and (b) body mass 102 kg, the transmissibility curves of passive seat suspension for excitation signals: (c) WNP, (e) EM3 and of active seat suspension for excitation signals: (d) WNP, (f) EM3, body mass 55 kg (—) and 102 kg (-·-·-).

5. Laboratory experimental results

The experimental investigations were performed using the same test set-up that has been described in Section 2.4. The electro-hydraulic shaker was utilised as an actuator that provided a random vibration source for testing and analysis. Two high output linear accelerometers were installed in order to measure the vibration of the shaker and the suspended body. Additionally, the cable extension position sensor was installed for measuring the relative displacement of the suspension system. PC-based data acquisition system was used as a combination of modular hardware, application software, and a computer to take measurements. The measurement results were reported for a mass-loaded suspension system mechanism. In that case, a seat cushion was removed and a metal mass-load was mounted rigidly on the suspension system.

The transmissibility curves of the passive and active suspension systems for the different values of mass: m=50, 80 and 120 kg were shown in Fig. 11. The dynamic behaviour of the active system loaded by the two different masses was nearly the same in the frequency range 0.5–4 Hz. This was desirable for seat design as the variable mass of the machine operators did not influence its performance. The system robustness at the higher frequency range was not improved by the active control. Different load masses affected the dynamic response of the active suspension system in the frequency range higher than 4 Hz and the seat suspension dynamic behaviour was more similar to the passive system.

In this paper, the object of vibration isolation was assumed as the lumped mass body. That did not reflect all the properties of a real, complex vibration isolated system such as a human operator body seated on the cushion. It is obvious that the dynamics of the cushion and the operator can affect the seat suspension performance. However, such assumption made the experimental investigations repeatable and, in consequence, the measured and computed results could be compared more precisely. For example, differences in the posture of seated person can cause a 10 percent difference in test results [31]. Moreover, the height and mass distribution of a tested person cause the disturbances in test results, making such investigations hardly ever repeatable. Additionally, the transmissibility behaviour of the seat suspension loaded by the pure mass and a human body was similar in the vertical direction. In order to prove that the obtained results have been acceptable to get a final conclusion, a test with a test person of the passive and active seats was performed additionally. The experimental set-up and transmissibility curves for the light and heavy persons were presented in Fig. 12.

The presented results show that the vibro-isolation properties of the seat were significantly improved by the active control. The required system robustness of the active seat in response to varying load mass was still achieved (Fig. 12d, f). In the case of the passive seat, different load masses affected its dynamic response and high amplification of the resonance amplitude was observed for that system (Fig. 12c, e).

6. Conclusions

The active control of the air-flow to the air-spring resulted in a reduction of the amplitude at resonance by about 50 percent in comparison to the passive system. Additionally, the high system robustness of the actively controlled suspension in response to varying load mass was achieved in the 0.5–4 Hz frequency range. In that frequency range the air-flow effectively controlled the air-spring force. The passive and active seat suspensions showed similar behaviour at higher frequencies, because at higher frequencies (more than 4 Hz) the shock-absorber force and the friction force were dominant. Besides, the active system was too slow for the higher frequency vibration, therefore its efficiency was lower.

The Seat Effective Amplitude Transmissibility factor (SEAT) for the active seat was significantly lower than for the passive system. The reduction of the conflicting maximum relative displacement of the active system was observed for high suspension load masses. Moreover, the desirable system robustness of the active seat for different load masses of suspension system was achieved. The advantages of the active system: the more effective vibration control in the low frequency range and the higher robustness to driver's mass variations made the active suspension system worthwhile to be used in engineering practice. The better vibration control properties of the active system in respect of the passive one and its better robustness to load mass variations were demonstrated by simulation and experimental studies. The experimental results, both with the dummy masses and two test persons, demonstrated the realistic advantages of the active system, at least for the EM3 excitation signal. That was the essence of the importance and novelty of the paper. Showing the prospect of practical application of active pneumatic suspension system in the search after higher comfort and less potential health problems of the workers is a new contribution in the field of seating dynamics research.

In the future work, optimal controller settings for the active seat suspension system with a triple feedback loop should be found. The multicriteria optimisation might effectively help to obtain the best vibro-isolating properties of the suspension system. The optimal controller settings must ensure the minimisation of the dynamic forces transmitted from the cabin's floor to the seat and the minimisation of the suspension deflection in order to ensure the controllability of working machines (these are opposing criteria). Additionally, the system robustness in response to the load mass and other operational variables criterion should be included in the optimisation procedure.

Acknowledgements

This work was supported by the Polish Ministry of Science and Higher Education research Grant (Project no. N N501 326135, years: 2008–2010). We would like to thank Isringhausen GMBH and CO. KG for the assistance in the experimental research.

Appendix A. Parameter values used by the seat suspension model

Each parameter value used by the seat suspension model was shown in Table A1.

Table A1

	Passive	Active	Unit
Surface of the air-spring (A_{as})	0.1	0.1	m^2
Effective area of the air-spring (A_{ef})	7.164×10^{-3}	7.164×10^{-3}	m^2
Critical pressure ratio (b)	0.12	0.12	
Gravity constant (g)	9.81	9.81	m/s^2
Initial height of the air-spring (h_0)	0.042	0.042	m

Table A1 (*continued*)

	Passive	Active	Unit
Static gain of the control valve (k_s)	1.65×10^{-8}	1.65×10^{-8}	$m^3/(s\,Pa\,V)$
Proportional gain of the acceleration control loop (K_1)	0	0.4	$V\,s^2/m$
Proportional gain of the relative velocity control loop (K_2)	0	2.222	$V\,s/m$
Proportional gain of the relative displacement control loop (K_3)	0	4.444	V/m
Nominal value of the suspended mass ($\overline{m}$)	100	100	kg
Mass of suspension system affixed to suspended mass (m_s)	7	7	kg
Air pressure of the power supply (p_s)	9×10^5	9×10^5	Pa
Atmospheric pressure (p_0)	1×10^5	1×10^5	Pa
Gas constant (R)	287	287	J/(kg K)
Time constant of the control valve (t_0)	0.01	0.01	s
Air temperature of the power supply (T_s)	293	293	K
Temperature of standard conditions (T_{norm})	293	293	K
Wall temperature of the air-spring (T_w)	293	293	K
Atmospheric air temperature (T_0)	293	293	K
Maximum value of the overall control voltage (u_{max})	1	1	V
Minimum value of the overall control voltage (u_{min})	-1	-1	V
Setting value of the acceleration control loop ($\ddot{x}_{set}$)	0	0	m/s^2
Setting value of the relative displacement control loop ($(x-x_s)_{set}$)	0.135	0.135	m
Setting value of the relative velocity control loop ($(\dot{x}-\dot{x}_s)_{set}$)	0	0	m/s
Overall heat transfer coefficient of the air-spring (α_{as})	25	25	$W/(m^2\,K)$
Variations of the value of suspended mass (Δ_m)	±0.5	±0.5	
Reduction ratio of the air-spring (δ_{as})	2.88	2.88	
Adiabatic coefficient (κ)	1.4	1.4	
Density of standard conditions (ρ_{norm})	1.293	1.293	kg/m^3

References

[1] D. Karnopp, Analytical results for optimum actively damped suspensions under random excitation, *ASME Journal of Vibration, Acoustics, Stress and Reliability in Design* 111 (1989) 278–283.
[2] A.G. Thompson, Optimum damping in a randomly excited non-linear suspension, *Proceedings of the Institution of Mechanical Engineers* 184 (1969) 169–184.
[3] D.A. Crolla, Semi-active suspension control for a full vehicle model, *SAE Technical Paper Series* 911904 (1992) 45–51.
[4] R.M. Goodall, W. Kortüm, Active control in ground transportation—review of the state-of-the-art and future potential, *Vehicle System Dynamics* 12 (1983) 225–257.
[5] D. Hrovat, Optimal active suspensions for 3d vehicle models, *Proceedings of the American Control Conference*, Vol. 2, AZ, USA, 1991, pp. 1534–1541.
[6] G.J. Stein, Results of investigation of an electro-pneumatic active vibration control system, *Proceedings of the Institution of Mechanical Engineers Part D: Journal of Automotive Engineering* 209 (1995) 227–234.
[7] J. Stein, I. Ballo, M. Gajarsky, Active vibration control system for driver'sseat, *25th ISATA Silver Jubilee International Symposium on Automotive Technology and Automation*, Automotive Automation Limited, Croydon, 1992, pp. 183–190.
[8] R.S. Sharp, J.H. Hassan, Performance predictions for a pneumatic active car suspension system, *Proceedings of the Institution of Mechanical Engineers Part D: Journal of Automotive Engineering* 202 (D4) (1988) 241–250.
[9] D. Cho, J.K. Hedrick, Pneumatic actuators for vehicle active suspension applications, *Journal of Dynamical System, Measurement and Control* 107 (3) (1985) 67–72.
[10] L. Benassi, S.J. Elliott, P. Gardonio, Active vibration isolation using an inertial actuator with local force feedback control, *Journal of Sound and Vibration* 276 (2004) 157–179.
[11] T.P. Gunston, J. Rebelle, M.J. Griffin, A comparison of two methods of simulating seat suspension dynamic performance, *Journal of Sound and Vibration* 278 (2004) 117–134.
[12] C.-M. Lee, A.H. Bogatchenkov, V.N. Goverdovskiy, Y.V. Shynkarenko, A.I. Temnikov, Position control of seat suspension with minimum stiffness, *Journal of Sound and Vibration* 292 (2006) 435–442.
[13] G. Stein, New results on an electropneumatic active seat suspension system, *Proceedings of the Institution of Mechanical Engineers, Part D: Journal of Automobile Engineering* 214 (5) (2000) 533–544.
[14] G. Stein, Hybrid control system for an AVC unit, *Archives of Control Sciences* 13 (XLIX) (2003) 157–175.
[15] J.D. Wu, R.J. Chen, Application of an active controller for reducing small-amplitude vertical vibration in a vehicle seat, *Journal of Sound and Vibration* 274 (2004) 939–951.
[16] J.K. Hedrick, D.N. Wormley, Active suspension foreground transport vehicles—a state of the art review, *Transactions of the American Society of Mechanical Engineers, Monograph, Mechanical of Transportation Systems* AMD15 (1975).
[17] C. Yue, T. Butsen, K. Hedrick, Alternative control laws for automotive active suspensions, *Transactions of the American Society of Mechanical Engineers, Journal of Dynamic Systems, Measurement and Control* 111 (1989) 175–180.
[18] M.N. Khajavi, V. Abdollahi, Comparison between optimized passive vehicle suspension system and semi active fuzzy logic controlled suspension system regarding ride and handling, *Proceedings of World Academy of Science, Engineering and Technology*, Vol. 21, 2007.
[19] T. Yoshimura, K. Nakaminami, M. Kurimoto, J. Hino, Active suspension of passenger cars using linear and fuzzy-logic controls, *Control Engineering Practice* 7 (1999) 41–47.
[20] Y. Watanabe, R.S. Sharp, Neural network learning control of automotive active suspension systems, *International Journal of Vehicle Design* 21 (2–3) (2004) 124–147.
[21] S. Yildirim, Vibration control of suspension systems using a proposed neural network, *Journal of Sound and Vibration* 277 (2004) 1059–1069.
[22] H. Du, K.Y. Sze, J. Lam, Semi-active H-inf control of vehicle suspension with magneto-rheological dampers, *Journal of Sound and Vibration* 283 (2005) 981–996.
[23] H. Du, N. Zhang, H-inf control of active vehicle suspension with actuator time delay, *Journal of Sound and Vibration* 301 (2007) 236–252.

[24] Y. He, J. McPhee, Multidisciplinary design optimization of mechatronic vehicles with active suspensions, *Journal of Sound and Vibration* 283 (2005) 217–241.
[25] I. Maciejewski, L. Meyer, T. Krzyzynski, Modelling and multi-criteria optimisation of passive seat suspension vibro-isolating properties, *Journal of Sound and Vibration* 324 (2009) 520–538.
[26] P. Beater, *Pneumatic Drives, System Design, Modelling and Control*, Springer-Verlag, Berlin, Heidelberg, 2007.
[27] E.W. Gerc, *Pneumatic Drives, Theory, and Calculation*, WNT, Warsaw, 1973 (in Polish).
[28] International Organization for Standarization, Pneumatic fluid power—components using compressible fluids—determination of flow-rate characteristics, ISO 6358, Geneva, 1989.
[29] A. Preumont, *Vibration Control of Active Structures: An Introduction*, Kluwer Academic Publishers, London, 2002.
[30] P. Bogacki, L.F. Shampine, A 3(2) pair of Runge–Kutta formulas, *Applied Mathematics Letters* 2 (4) (1989) 321–325.
[31] International Organization for Standarization, Earth-moving machinery—laboratory evaluation of operator seat vibration, ISO 7096, Geneva, 2000.
[32] International Organization for Standarization, Mechanical vibration and shock—evolution of human exposure to whole-body vibration, ISO 2631, Geneva, 1997.
[33] M.J. Griffin, *Handbook of Human Vibration*, London, 1996.
[34] D. Gu, P. Petkov, M. Konstantinov, *Robust Control Design with MATLAB*, Springer, Berlin, 2005.